

# Measurement of the Branching Fractions for $J/\psi \rightarrow p\bar{p}\eta$ and $p\bar{p}\eta'$

M. Ablikim<sup>1</sup>, J. Z. Bai<sup>1</sup>, Y. Bai<sup>1</sup>, Y. Ban<sup>11</sup>, X. Cai<sup>1</sup>, H. F. Chen<sup>16</sup>, H. S. Chen<sup>1</sup>, H. X. Chen<sup>1</sup>, J. C. Chen<sup>1</sup>, Jin Chen<sup>1</sup>, X. D. Chen<sup>5</sup>, Y. B. Chen<sup>1</sup>, Y. P. Chu<sup>1</sup>, Y. S. Dai<sup>18</sup>, Z. Y. Deng<sup>1</sup>, S. X. Du<sup>1a</sup>, J. Fang<sup>1</sup>, C. D. Fu<sup>1</sup>, C. S. Gao<sup>1</sup>, Y. N. Gao<sup>14</sup>, S. D. Gu<sup>1</sup>, Y. T. Gu<sup>4</sup>, Y. N. Guo<sup>1</sup>, Z. J. Guo<sup>15b</sup>, F. A. Harris<sup>15</sup>, K. L. He<sup>1</sup>, M. He<sup>12</sup>, Y. K. Heng<sup>1</sup>, H. M. Hu<sup>1</sup>, T. Hu<sup>1</sup>, G. S. Huang<sup>1c</sup>, X. T. Huang<sup>12</sup>, Y. P. Huang<sup>1</sup>, X. B. Ji<sup>1</sup>, X. S. Jiang<sup>1</sup>, J. B. Jiao<sup>12</sup>, D. P. Jin<sup>1</sup>, S. Jin<sup>1</sup>, G. Li<sup>1</sup>, H. B. Li<sup>1</sup>, J. Li<sup>1</sup>, L. Li<sup>1</sup>, R. Y. Li<sup>1</sup>, W. D. Li<sup>1</sup>, W. G. Li<sup>1</sup>, X. L. Li<sup>1</sup>, X. N. Li<sup>1</sup>, X. Q. Li<sup>10</sup>, Y. F. Liang<sup>13</sup>, B. J. Liu<sup>1d</sup>, C. X. Liu<sup>1</sup>, Fang Liu<sup>1</sup>, Feng Liu<sup>6</sup>, H. M. Liu<sup>1</sup>, J. P. Liu<sup>17</sup>, H. B. Liu<sup>4e</sup>, J. Liu<sup>1</sup>, Q. Liu<sup>15</sup>, R. G. Liu<sup>1</sup>, S. Liu<sup>8</sup>, Z. A. Liu<sup>1</sup>, F. Lu<sup>1</sup>, G. R. Lu<sup>5</sup>, J. G. Lu<sup>1</sup>, C. L. Luo<sup>9</sup>, F. C. Ma<sup>8</sup>, H. L. Ma<sup>2</sup>, Q. M. Ma<sup>1</sup>, M. Q. A. Malik<sup>1</sup>, Z. P. Mao<sup>1</sup>, X. H. Mo<sup>1</sup>, J. Nie<sup>1</sup>, S. L. Olsen<sup>15</sup>, R. G. Ping<sup>1</sup>, N. D. Qi<sup>1</sup>, J. F. Qiu<sup>1</sup>, G. Rong<sup>1</sup>, X. D. Ruan<sup>4</sup>, L. Y. Shan<sup>1</sup>, L. Shang<sup>1</sup>, C. P. Shen<sup>15</sup>, X. Y. Shen<sup>1</sup>, H. Y. Sheng<sup>1</sup>, H. S. Sun<sup>1</sup>, S. S. Sun<sup>1</sup>, Y. Z. Sun<sup>1</sup>, Z. J. Sun<sup>1</sup>, X. Tang<sup>1</sup>, J. P. Tian<sup>14</sup>, G. L. Tong<sup>1</sup>, G. S. Varner<sup>15</sup>, X. Wan<sup>1</sup>, L. Wang<sup>1</sup>, L. L. Wang<sup>1</sup>, L. S. Wang<sup>1</sup>, P. Wang<sup>1</sup>, P. L. Wang<sup>1</sup>, Y. F. Wang<sup>1</sup>, Z. Wang<sup>1</sup>, Z. Y. Wang<sup>1</sup>, C. L. Wei<sup>1</sup>, D. H. Wei<sup>3</sup>, N. Wu<sup>1</sup>, X. M. Xia<sup>1</sup>, G. F. Xu<sup>1</sup>, X. P. Xu<sup>6</sup>, Y. Xu<sup>10</sup>, M. L. Yan<sup>16</sup>, H. X. Yang<sup>1</sup>, M. Yang<sup>1</sup>, Y. X. Yang<sup>3</sup>, M. H. Ye<sup>2</sup>, Y. X. Ye<sup>16</sup>, C. X. Yu<sup>10</sup>, C. Z. Yuan<sup>1</sup>, Y. Yuan<sup>1</sup>, Y. Zeng<sup>7</sup>, B. X. Zhang<sup>1</sup>, B. Y. Zhang<sup>1</sup>, C. C. Zhang<sup>1</sup>, D. H. Zhang<sup>1</sup>, H. Q. Zhang<sup>1</sup>, H. Y. Zhang<sup>1</sup>, J. W. Zhang<sup>1</sup>, J. Y. Zhang<sup>1</sup>, X. Y. Zhang<sup>12</sup>, Y. Y. Zhang<sup>13</sup>, Z. X. Zhang<sup>11</sup>, Z. P. Zhang<sup>16</sup>, D. X. Zhao<sup>1</sup>, J. W. Zhao<sup>1</sup>, M. G. Zhao<sup>1</sup>, P. P. Zhao<sup>1</sup>, Z. G. Zhao<sup>16</sup>, B. Zheng<sup>1</sup>, H. Q. Zheng<sup>11</sup>, J. P. Zheng<sup>1</sup>, Z. P. Zheng<sup>1</sup>, B. Zhong<sup>9</sup>, L. Zhou<sup>1</sup>, K. J. Zhu<sup>1</sup>, Q. M. Zhu<sup>1</sup>, X. W. Zhu<sup>1</sup>, Y. S. Zhu<sup>1</sup>, Z. A. Zhu<sup>1</sup>, Z. L. Zhu<sup>3</sup>, B. A. Zhuang<sup>1</sup>, B. S. Zou<sup>1</sup>

(BES Collaboration)

<sup>1</sup> *Institute of High Energy Physics, Beijing 100049, People's Republic of China*

<sup>2</sup> *China Center for Advanced Science and Technology (CCAST),  
Beijing 100080, People's Republic of China*

<sup>3</sup> *Guangxi Normal University, Guilin 541004, People's Republic of China*

- <sup>4</sup> *Guangxi University, Nanning 530004, People's Republic of China*
- <sup>5</sup> *Henan Normal University, Xinxiang 453002, People's Republic of China*
- <sup>6</sup> *Huazhong Normal University, Wuhan 430079, People's Republic of China*
- <sup>7</sup> *Hunan University, Changsha 410082, People's Republic of China*
- <sup>8</sup> *Liaoning University, Shenyang 110036, People's Republic of China*
- <sup>9</sup> *Nanjing Normal University, Nanjing 210097, People's Republic of China*
- <sup>10</sup> *Nankai University, Tianjin 300071, People's Republic of China*
- <sup>11</sup> *Peking University, Beijing 100871, People's Republic of China*
- <sup>12</sup> *Shandong University, Jinan 250100, People's Republic of China*
- <sup>13</sup> *Sichuan University, Chengdu 610064, People's Republic of China*
- <sup>14</sup> *Tsinghua University, Beijing 100084, People's Republic of China*
- <sup>15</sup> *University of Hawaii, Honolulu, HI 96822, USA*
- <sup>16</sup> *University of Science and Technology of  
China, Hefei 230026, People's Republic of China*
- <sup>17</sup> *Wuhan University, Wuhan 430072, People's Republic of China*
- <sup>18</sup> *Zhejiang University, Hangzhou 310028, People's Republic of China*
- <sup>a</sup> *Current address: Zhengzhou University, Zhengzhou 450001, People's Republic of China*
- <sup>b</sup> *Current address: Johns Hopkins University, Baltimore, MD 21218, USA*
- <sup>c</sup> *Current address: University of Oklahoma, Norman, Oklahoma 73019, USA*
- <sup>d</sup> *Current address: University of Hong Kong, Pok Fu Lam Road, Hong Kong*
- <sup>e</sup> *Current address: Graduate University of Chinese Academy  
of Sciences, Beijing 100049, People's Republic of China*

## Abstract

Using  $58 \times 10^6$   $J/\psi$  events collected with the Beijing Spectrometer (BESII) at the Beijing Electron Positron Collider (BEPC), the branching fractions of  $J/\psi$  to  $p\bar{p}\eta$  and  $p\bar{p}\eta'$  are determined. The ratio  $\frac{\Gamma(J/\psi \rightarrow p\bar{p}\eta)}{\Gamma(J/\psi \rightarrow p\bar{p})}$  obtained by this analysis agrees with expectations based on soft-pion theorem calculations.

PACS numbers:

## I. INTRODUCTION

The  $J/\psi$  meson has hadronic, electromagnetic, and radiative decays to light hadrons, and a radiative transition to the  $\eta_c$ . In Ref. [1], direct hadronic, electromagnetic and radiative decays are estimated to account for 69.2%, 13.4%, and 4.3%, respectively, of all  $J/\psi$  decays. However, individual exclusive  $J/\psi$  decays are more difficult to analyze quantitatively in QCD. To date, two-body decay modes such as  $J/\psi \rightarrow B_8 \bar{B}_8$  or  $P_9 V_9$ , where  $B_8$ ,  $P_9$  and  $V_9$  refer to baryon octet, pseudoscalar nonet, and vector nonet particle, respectively, have been studied with some success using an effective model, and other similar methods [2].

Studies of three-body decays of  $J/\psi$  are a natural extension of studies of two-body decays. Since most  $J/\psi$  decays proceed via two-body intermediate states, including wide resonances, it is hard to experimentally extract the non-resonant three-body contribution [3]. Specific models based on proton and  $N^*$  pole diagrams have been introduced to deal with these problems [2]. In the calculation, the soft-pion theorem [4] has been applied to the decay  $J/\psi \rightarrow p\bar{p}\pi^0$  successfully. This method has also been used for  $J/\psi \rightarrow p\bar{p}\eta$  and  $J/\psi \rightarrow p\bar{p}\eta'$  decays [2].

This paper reports measurement of the branching fractions for  $p\bar{p}\eta$  and  $p\bar{p}\eta'$ , and tests of the soft-pion theorem for  $J/\psi \rightarrow p\bar{p}\eta$ , which states [2]:

$$\frac{\Gamma(J/\psi \rightarrow p\bar{p}\eta)}{\Gamma(J/\psi \rightarrow p\bar{p})} \simeq 0.64 \pm 0.52.$$

## II. THE BES DETECTOR AND MONTE CARLO SIMULATION

BESII is a conventional solenoidal magnet detector that is described in detail in Refs. [5]. A 12-layer vertex chamber (VC) surrounding the beam pipe provides trigger and track information. A forty-layer main drift chamber (MDC), located radially outside the VC, provides trajectory and energy loss ( $dE/dx$ ) information for tracks over 85% of the total solid angle. The momentum resolution is  $\sigma_p/p = 0.017\sqrt{1+p^2}$  ( $p$  in GeV/ $c$ ), and the  $dE/dx$  resolution for hadron tracks is  $\sim 8\%$ . An array of 48 scintillation counters surrounding the MDC measures the time-of-flight (TOF) of tracks with a resolution of

$\sim 200$  ps for hadrons. Radially outside the TOF system is a 12 radiation length, lead-gas barrel shower counter (BSC). This measures the energies of electrons and photons over  $\sim 80\%$  of the total solid angle with an energy resolution of  $\sigma_E/E = 22\%/\sqrt{E}$  ( $E$  in GeV). Outside of the solenoidal coil, which provides a 0.4 Tesla magnetic field over the tracking volume, is an iron flux return that is instrumented with three double layers of counters that identify muons of momentum greater than 0.5 GeV/ $c$ .

In the analysis, a GEANT3-based Monte Carlo (MC) simulation program (SIMBES) [6] with detailed consideration of detector performance is used. The consistency between data and MC has been validated using many high purity physics channels [7].

In this analysis, the detection efficiency for each decay mode is determined by a MC simulation that takes into account the angular distributions. For  $J/\psi \rightarrow p\bar{p}\eta$ , the angle ( $\theta$ ) between the directions of  $e^+$  and  $p$  in the laboratory frame is generated according to  $1 + \alpha \cdot \cos^2\theta$  distribution, where  $\alpha$  is obtained by fitting the data from  $J/\psi \rightarrow p\bar{p}\eta$ . A uniform phase space distribution is used for  $J/\psi$  decaying into  $p\bar{p}\eta'$ .

### III. GENERAL SELECTION CRITERIA

Candidate events are required to satisfy the following common selection criteria:

#### A. Charged track selection

Each charged track must: (1) have a good helix fit in order to ensure a correct error matrix in the kinematic fit; (2) originate from the interaction region,  $\sqrt{V_x^2 + V_y^2} < 2$  cm and  $|V_z| < 20$  cm, where  $V_x$ ,  $V_y$ , and  $V_z$  are the  $x$ ,  $y$  and  $z$  coordinates of the point of closest approach of the track to the beam axis; (3) have a transverse momentum greater than 70 MeV/ $c$ ; and (4) have  $|\cos\theta| \leq 0.80$ , where  $\theta$  is the polar angle of the track.

## B. Photon selection

A neutral cluster in the BSC is assumed to be a photon candidate if the following requirements are satisfied: (1) the energy deposited in the BSC is greater than 0.05 GeV; (2) energy is deposited in more than one layer; (3) the angle between the direction of photon emission and the direction of shower development is less than  $30^\circ$ ; and (4) the angle between the photon and the nearest charged track is greater than  $5^\circ$  (if the charged track is an antiproton, the angle is required to be greater than  $25^\circ$ ).

## C. Particle Identification (PID)

For each charged track in an event,  $\chi_{PID}^2(i)$  is determined using both  $dE/dx$  and TOF information:

$$\chi_{PID}^2(i) = \chi_{dE/dx}^2(i) + \chi_{TOF}^2(i),$$

where  $i$  corresponds to the particle hypothesis. A charged track is identified as a pion if  $\chi_{PID}^2$  for the  $\pi$  hypothesis is less than those for the kaon and proton hypotheses. For  $p$  or  $\bar{p}$  identification, the same method is used. In this analysis, all charged tracks are required to be positively identified.

## IV. ANALYSIS OF $J/\psi \rightarrow p\bar{p}\eta$

The decay modes for the  $J/\psi \rightarrow p\bar{p}\eta$  measurement are  $\eta \rightarrow \gamma\gamma$  and  $\eta \rightarrow \pi^+\pi^-\pi^0$ . The use of different decay modes allows us to cross check our measurements, as well as to obtain higher statistical precision.

### A. $\eta \rightarrow \gamma\gamma$

Events with two charged tracks and two photons are selected. A four-constraint (4C) kinematic fit is performed to the hypothesis  $J/\psi \rightarrow p\bar{p}\gamma\gamma$ . For events with more than two

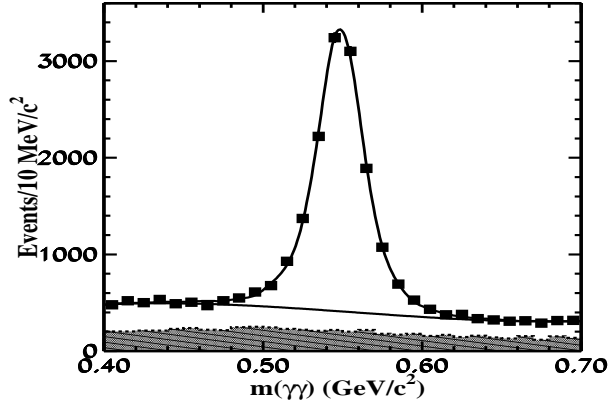


FIG. 1: The two-photon invariant mass distribution for  $J/\psi \rightarrow p\bar{p}\gamma\gamma$  candidate events. Data are represented by rectangles; the error bars are too small to be seen. The curves are the results of the fit described in the text. The shaded part is background from MC simulation.

photons, all combinations are tried, and the combination with the smallest  $\chi^2$  is retained.  $\chi^2_{\gamma\gamma p\bar{p}}$  is required to be less than 20.

The  $\gamma\gamma$  invariant mass ( $m_{\gamma\gamma}$ ) distribution for selected events is shown in Fig. 1. A peak around the  $\eta$  mass is evident. The curves in the figure indicate the best fit to the signal and background. The shaded part is the background estimated from a MC simulation of inclusive  $J/\psi$  events [8]. The main background comes from  $J/\psi \rightarrow p\bar{p}\pi^0\pi^0$  and  $\Sigma^+\bar{\Sigma}^-$ . By fitting the  $\eta$  signal with a MC-simulated signal histogram plus a third order polynomial background function, the number of  $\eta$  signal events is determined to be  $(12220 \pm 149)$ .

For the signal MC simulation, the events are generated with a proton angle distribution of  $1 + \alpha \cos^2 \theta$ , where  $\alpha$  is taken to be -0.6185 in order to describe the data. In the decay, intermediate resonances, N(1440), N(1535), N(1650), and N(1800) and antiparticles, with fractional contribution of  $(8 \pm 4)\%$ ,  $(56 \pm 15)\%$ ,  $(24^{+5}_{-15})\%$ , and  $(12 \pm 7)\%$  [9], respectively, are included. The resulting detection efficiency for  $J/\psi \rightarrow p\bar{p}\eta$  ( $\eta \rightarrow \gamma\gamma$ ) is determined to be 28.70%. The  $p\bar{p}\eta$  branching fraction, calculated using

$$B(J/\psi \rightarrow p\bar{p}\eta) = \frac{N_{obs}}{\epsilon \cdot N_{J/\psi} \cdot B(\eta \rightarrow 2\gamma) \cdot f_1},$$

is  $(1.93 \pm 0.02) \times 10^{-3}$ , where the error is statistical only. Here  $N_{obs}$  represents the number of observed events,  $\epsilon$  is the detection efficiency for  $J/\psi \rightarrow p\bar{p}\eta(\eta \rightarrow 2\gamma)$ ,  $f_1 = 0.9739$  is the

efficiency correction factor (see Section VI), and  $N_{J/\psi}$  is the total number of  $J/\psi$  events.

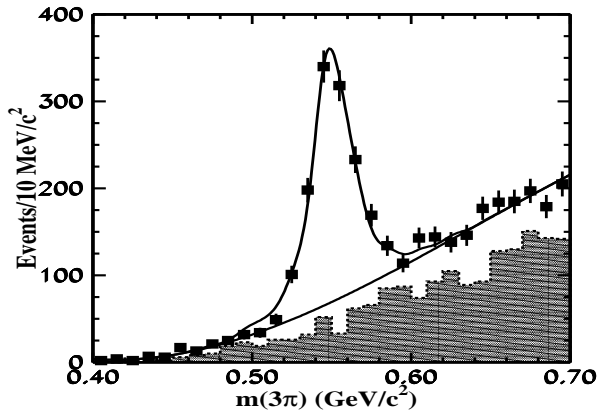


FIG. 2: The  $\pi^+\pi^-\pi^0$  invariant mass distribution for  $J/\psi \rightarrow p\bar{p}\pi^+\pi^-\pi^0$  candidate events. The curves are results of the fit described in the text. The shaded part is background from MC simulation.

### B. $\eta \rightarrow \pi^+\pi^-\pi^0$

Similar to the above analysis, events with four charged tracks and two photons are selected. A 4C kinematic fit is performed to the  $J/\psi \rightarrow p\bar{p}\pi^+\pi^-\gamma\gamma$  hypothesis, and the  $\chi^2_{\gamma\gamma p\bar{p}\pi^+\pi^-}$  value is required to be less than 20. In order to suppress multi-photon backgrounds, the number of photons is required to be two. The invariant mass of the  $\gamma\gamma$  is required to be between 0.095 and 0.175  $\text{GeV}/c^2$ .

The  $\pi^+\pi^-\pi^0$  invariant mass ( $m_{\pi^+\pi^-\pi^0}$ ) distribution is shown in Fig. 2, where a peak at the  $\eta$  mass is observed. The curves in the figure are the results of a fit to the signal and background. The shaded part is background estimated from MC simulation of inclusive  $J/\psi$  decay events [8]. Here the main background comes from  $J/\psi \rightarrow p\bar{p}\pi^+\pi^-\pi^0$  and  $p\bar{p}\pi^+\pi^-\gamma$  decays. By fitting the distribution with a MC simulated signal histogram plus a third order polynomial background function,  $(954 \pm 45)$  signal events are obtained. Similar to the  $\eta \rightarrow 2\gamma$  decay, contributions from the baryon excited states N(1440), N(1535), N(1650), and N(1800), as well as their anti-particles [9], are considered. The detection efficiency of  $J/\psi \rightarrow p\bar{p}\eta$  ( $\eta \rightarrow \pi^+\pi^-\pi^0$ ,  $\pi^0 \rightarrow \gamma\gamma$ ) is determined to be 4.20%.

The branching fraction is determined from the calculation

$$B(J/\psi \rightarrow p\bar{p}\eta) = \frac{N_{obs}}{\epsilon \cdot N_{J/\psi} \cdot B(\eta \rightarrow \pi^+\pi^-\pi^0)} \cdot \frac{1}{B(\pi^0 \rightarrow \gamma\gamma) \cdot f_2},$$

where  $f_2 = 0.9582$  is a correction factor for the efficiency that is described below in Section VI. We determine a branching fraction for  $J/\psi \rightarrow p\bar{p}\eta$  of  $(1.83 \pm 0.09) \times 10^{-3}$ , where the error is statistical only.

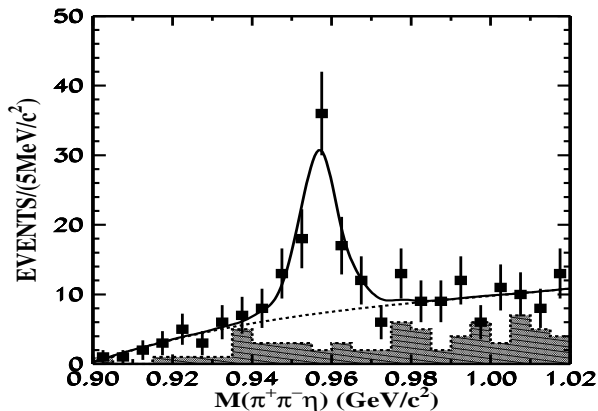


FIG. 3: The  $\pi^+\pi^-\eta$  invariant mass distribution for  $J/\psi \rightarrow p\bar{p}\pi^+\pi^-\eta$  candidate events. The curves are results of the fit described in the text. The shaded part is background from MC simulation.

## V. ANALYSIS OF $J/\psi \rightarrow p\bar{p}\eta'$

There are three main decay modes of the  $\eta'$ :  $\eta' \rightarrow \pi^+\pi^-\eta$ ,  $\eta' \rightarrow \gamma\rho^0$  and  $\eta' \rightarrow \pi^0\pi^0\eta$ . Here the first two decay modes are used.

### A. $\eta' \rightarrow \pi^+\pi^-\eta$ , $\eta \rightarrow \gamma\gamma$

In the search for  $\eta' \rightarrow \pi^+\pi^-\eta$  decays, events with four charged tracks and two photons are selected. A five-constraint (5C) kinematic fit is performed to the hypothesis of  $J/\psi \rightarrow$

$p\bar{p}\pi^+\pi^-\gamma\gamma$ , in which the  $2\gamma$  invariant mass is constrained to equal the  $\eta$  mass, and the  $\chi^2_{\gamma\gamma p\bar{p}\pi^+\pi^-}$  value is required to be less than 20.

The  $\pi^+\pi^-\eta$  invariant mass ( $m_{\pi^+\pi^-\eta}$ ) distribution for events that survive the selection criteria is shown in Fig. 3. A clear  $\eta'$  signal is observed. The curves in the figure are the best fit to the signal and background. The shaded part is background estimated from MC simulation of inclusive  $J/\psi$  decay events [8]. The main background comes from  $J/\psi \rightarrow \Delta^+\bar{\Delta}^-\eta$ , and  $\Delta^0\bar{\Delta}^0\eta$  decays. By fitting the distribution with a MC simulated signal histogram plus a third order polynomial background function, a signal yield of  $(65 \pm 12)$  events is observed. According to a MC simulation, in which the events are generated with uniform phase space, the detection efficiency of  $J/\psi \rightarrow p\bar{p}\eta'$  ( $\eta' \rightarrow \pi^+\pi^-\eta$ ,  $\eta \rightarrow \gamma\gamma$ ) is 3.38%. The effect of intermediate resonances is considered as a source of systematic error. Using

$$B(J/\psi \rightarrow p\bar{p}\eta') = \frac{N_{obs}}{\epsilon \cdot N_{J/\psi} \cdot B(\eta' \rightarrow \pi^+\pi^-\eta)} \cdot \frac{1}{B(\eta \rightarrow \gamma\gamma) \cdot f_3}$$

with  $f_3 = 0.8228$  being the efficiency correction factor (see Section VI), we determine the branching fraction for  $J/\psi \rightarrow p\bar{p}\eta'$  to be  $(2.31 \pm 0.43) \times 10^{-4}$ , where the error is statistical only.

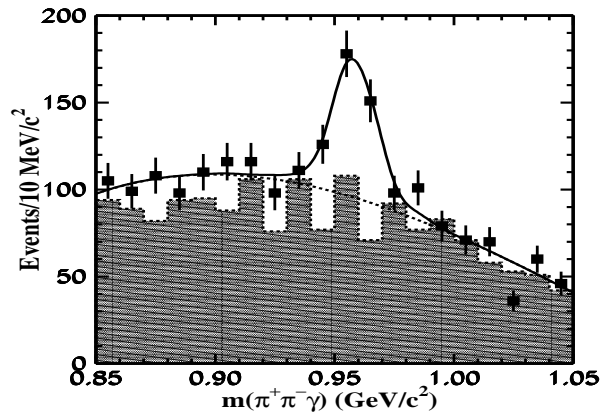


FIG. 4: The  $\gamma\pi^+\pi^-$  invariant mass distribution for  $J/\psi \rightarrow p\bar{p}\gamma\pi^+\pi^-$  candidate events. The curves are results of the fit described in the text. The shaded part is background from MC simulation.

## B. $\eta' \rightarrow \gamma\rho^0, \rho^0 \rightarrow \pi^+\pi^-$

In order to select  $\eta' \rightarrow \gamma\rho^0$ , a 4C kinematic fit is performed under the hypothesis of  $J/\psi \rightarrow p\bar{p}\pi^+\pi^-\gamma$ . The  $\chi^2_{\gamma p\bar{p}\pi^+\pi^-}$  value is required to be less than 20. To ensure the events are from  $\gamma\rho^0$ , a  $|m_{\pi^+\pi^-} - m_\rho| < 0.20 \text{ GeV}/c^2$  requirement is imposed, where  $m_{\pi^+\pi^-}$  is the  $\pi^+\pi^-$  invariant mass, and  $m_\rho$  is the  $\rho$  mass. In order to exclude the background from  $J/\psi \rightarrow p\bar{p}\pi^+\pi^-$ , it is required that the invariant mass of the four charged tracks is less than  $3.02 \text{ GeV}/c^2$ .

The  $\gamma\rho^0$  invariant mass ( $m_{\gamma\rho^0}$ ) distribution for selected events, where a clear  $\eta'$  signal is observed, is shown in Fig. 4. The curves in the figure are the best fit to the signal and background. The shaded part is the background estimated from MC simulation of inclusive  $J/\psi$  decay events [8]. The main background comes from  $J/\psi \rightarrow p\bar{p}\pi^+\pi^-\gamma$ ,  $\Delta^{++}\bar{\Delta}^{--}\pi^0$  and  $p\bar{p}\pi^+\pi^-\pi^0$  decays. By fitting the  $m_{\gamma\pi^+\pi^-}$  distribution with a MC simulated signal shape and a third order polynomial background function, we determine the number of  $\eta'$  signal events to be  $(200 \pm 29)$ . The detection efficiency for  $J/\psi \rightarrow p\bar{p}\eta'$  ( $\eta' \rightarrow \gamma\rho^0$ ) is determined to be 7.48%, assuming phase space production, where the  $\pi^+\pi^-$  mass distribution is generated according to measurements from  $J/\psi \rightarrow \phi\eta', \eta' \rightarrow \gamma\pi^+\pi^-$  [10]. Using

$$B(J/\psi \rightarrow p\bar{p}\eta') = \frac{N_{obs}}{\epsilon \cdot N_{J/\psi} \cdot B(\eta' \rightarrow \gamma\rho^0) \cdot f_4}$$

with the  $f_4$  correction factor of 0.8522 (see Section VI). The resulting branching fraction for  $J/\psi \rightarrow p\bar{p}\eta'$  is  $(1.85 \pm 0.27) \times 10^{-4}$ , where the error is statistical only.

TABLE I: Numbers used in the calculations of branching fractions and results.

Decay mode	$N_{obs}$	$\epsilon(\%)$	Branching fraction
$J/\psi \rightarrow p\bar{p}\eta, \eta \rightarrow \gamma\gamma$	$12220 \pm 149$	28.70	$B(J/\psi \rightarrow p\bar{p}\eta) = (1.93 \pm 0.02 \pm 0.18) \times 10^{-3}$
$J/\psi \rightarrow p\bar{p}\eta, \eta \rightarrow \pi^+\pi^-\pi^0$	$954 \pm 45$	4.20	$B(J/\psi \rightarrow p\bar{p}\eta) = (1.83 \pm 0.09 \pm 0.24) \times 10^{-3}$
$J/\psi \rightarrow p\bar{p}\eta', \eta' \rightarrow \pi^+\pi^-\eta$	$65 \pm 12$	3.38	$B(J/\psi \rightarrow p\bar{p}\eta') = (2.31 \pm 0.43 \pm 0.34) \times 10^{-4}$
$J/\psi \rightarrow p\bar{p}\eta', \eta' \rightarrow \gamma\rho^0$	$200 \pm 29$	7.48	$B(J/\psi \rightarrow p\bar{p}\eta') = (1.85 \pm 0.27 \pm 0.31) \times 10^{-4}$

## VI. SYSTEMATIC ERRORS

In our analysis, the systematic errors on the branching fractions come from the uncertainties in the MDC tracking, photon efficiency, particle identification, photon identification, kinematic fit, background shapes, hadronic interaction model, intermediate decay branching fraction, the  $\pi^0$  and  $\rho$  selection requirements, intermediate resonance states, and the total number of  $J/\psi$  events. The errors from the different sources are listed in Table II.

The MDC tracking efficiency has been measured using  $J/\psi \rightarrow \rho\pi$ ,  $\Lambda\bar{\Lambda}$ , and  $\psi(2S) \rightarrow \pi^+\pi^-J/\psi$ ,  $J/\psi$  to  $\mu^+\mu^-$ . The MC simulation agrees with data within 1 to 2% for each charged track [7]. Thus 4% is regarded as the systematic error for the two charged-track mode, and 8% for the four charged-track final states.

The photon detection efficiency has been studied using a sample of  $J/\psi \rightarrow \rho\pi$  [7] decays; the difference between data and MC simulation is about 2% for each photon. In this analysis, 2% is included in the systematic error for one-photon modes and 4% for two-photon modes.

The charged pion PID efficiency has been studied using  $J/\psi \rightarrow \rho\pi$  decays [7]. The PID efficiency from data is in good agreement with that from MC simulation with an average difference that is less than 1% for each charged pion. Here 2% is taken as the systematic error for identifying two pions.

The proton PID efficiencies have been studied using  $J/\psi \rightarrow p\bar{p}\pi^+\pi^-$  decays. The main difference between data and MC simulation occurs for tracks with momentum less than 0.35 GeV/c. We determine a weighting factor for identifying a proton or anti-proton as a function of momentum from studies of the  $J/\psi \rightarrow p\bar{p}\pi^+\pi^-$  channel. After considering the weight of each particle in an event, the difference between data and MC is determined to be  $\frac{\epsilon_{DT}}{\epsilon_{MC}} = 0.9739 \pm 0.0078$  for  $\eta \rightarrow 2\gamma$ ,  $0.9582 \pm 0.0199$  for  $\eta \rightarrow 3\pi$ ,  $0.8228 \pm 0.0211$  for  $\eta' \rightarrow \pi^+\pi^-\eta$ , and  $0.8522 \pm 0.0140$  for  $\eta' \rightarrow \gamma\rho^0$ . We take  $f_1 = 0.9739$ ,  $f_2 = 0.9582$ ,  $f_3 = 0.8228$ , and  $f_4 = 0.8522$  as efficiency correction factors for the corresponding decay channel, and 0.8%, 2.1%, 2.6%, and 1.6% are taken as the errors associated with identifying protons and anti-protons, respectively. The PID systematic errors for the four decay modes are listed in Table II.

For the systematic error of photon ID, which arises mainly from the simulation of fake photons,  $p\bar{p}$  and  $J/\psi \rightarrow p\bar{p}\pi^+\pi^-$  data samples were selected and  $10^5$  simulated  $p\bar{p}$  and  $J/\psi \rightarrow p\bar{p}\pi^+\pi^-$  events were generated, with real and fake photons. The decay mode  $J/\psi \rightarrow p\bar{p}$  is used for the photon ID systematic error of  $J/\psi \rightarrow p\bar{p}\eta$  ( $\eta \rightarrow 2\gamma$ ), and the decay mode  $J/\psi \rightarrow p\bar{p}\pi^+\pi^-$  for  $J/\psi \rightarrow p\bar{p}\eta$  ( $\eta \rightarrow 3\pi$ ) and  $J/\psi \rightarrow p\bar{p}\eta'$ . From the decay mode  $J/\psi \rightarrow p\bar{p}$ , the fake photon differences between data and MC is about 2.0%, while for the decay mode  $J/\psi \rightarrow p\bar{p}\pi^+\pi^-$ , the difference is 1.6%. Here 2.0% is taken as the systematic error associated with photon ID for the decay mode determined to be  $J/\psi \rightarrow p\bar{p}\eta$  ( $\eta \rightarrow \gamma\gamma$ ), and 1.6% for the decay modes  $J/\psi \rightarrow p\bar{p}\eta$  ( $\eta \rightarrow 3\pi$ ) and  $J/\psi \rightarrow p\bar{p}\eta'$ .

In Ref. [11], the uncertainty of the 4C kinematic fit is 4%, which we include here in the systematic error. The uncertainty of the 5C kinematic fit is 4.1% in Ref. [12]. Here we conservatively take 5% as the systematic error from the 5C kinematic fit for the decay mode  $\eta' \rightarrow \pi^+\pi^-\eta$ .

The systematic errors of the background uncertainty is obtained by changing the range of the fit and varying the order of the polynomial background. The errors range from 0.8% to 7.3% in all decay modes (see Table II for detail).

There are two models, FLUKA and GCALOR, used for simulating hadronic interactions; the different models lead to different detection efficiencies. The difference between them is regarded as a systematic error. For the decay  $J/\psi \rightarrow p\bar{p}\eta$  ( $\eta \rightarrow 2\gamma$ ), the difference is very small and negligible. For the other decay modes, it is about 1.4% for  $J/\psi \rightarrow p\bar{p}\eta$  ( $\eta \rightarrow \pi^+\pi^-\pi^0$ ),  $J/\psi \rightarrow p\bar{p}\eta'$  ( $\eta' \rightarrow \pi^+\pi^-\eta$ ), and 5.2% for  $J/\psi \rightarrow p\bar{p}\eta'$  ( $\eta' \rightarrow \gamma\rho^0$ ).

The branching fractions for the decays  $\pi^0 \rightarrow 2\gamma$ ,  $\eta \rightarrow 2\gamma$ ,  $\eta \rightarrow \pi^+\pi^-\pi^0$ ,  $\eta' \rightarrow \pi^+\pi^-\eta$ , and  $\eta' \rightarrow \gamma\rho$  are taken from the PDG [13]. The errors on these branching fractions are systematic errors in our measurements.

For the  $\eta \rightarrow 3\pi$  mode, the  $\pi^0$  mass is required to satisfy  $|M_{\gamma\gamma} - M_{\pi^0}| < 0.04 \text{ GeV}/c^2$ . To study the systematic error associated with this requirement,  $\pi^0$  samples are selected and simulated using  $J/\psi \rightarrow \rho\pi$ , and the data and MC efficiencies in the  $3\sigma$  signal region are compared with using the requirement or not, the difference is about 1%. Here it is taken as the systematic error caused by the  $\pi^0$  requirement.

For the  $\eta' \rightarrow \gamma\rho$  mode, we require that  $|M_{\pi^+\pi^-} - M_\rho| < 0.20 \text{ GeV}/c^2$ . According to Ref. [14], the uncertainty associated with this requirement is 5.9%. Here we take this as the systematic error for the  $\rho$  mass requirement.

In the signal MC simulation, we assume the presence of  $N(1440)$ ,  $N(1535)$ ,  $N(1650)$ , and  $N(1800)$  in the  $p\bar{p}\eta$  channel. If some of these resonances are not included, the efficiency of this channel changes. These differences are taken as the systematic error associated with possible intermediate states. The total systematic error associated with this is taken as the sum added in quadrature. For the decay modes with an  $\eta'$ , we take the difference in efficiency determined assuming the decay proceeds via an intermediate  $N(2090)$  resonance compared with phase space generation as the systematic error (see Table II for detail).

The uncertainty of the total number of  $J/\psi$  events is 4.7% [15]. Combining all errors in quadrature gives total systematic errors of 9.3% for  $\eta \rightarrow \gamma\gamma$ , 12.9% for  $\eta \rightarrow \pi^+\pi^-\pi^0$ , 14.8% for  $\eta' \rightarrow \pi^+\pi^-\eta$ , and 16.6% for  $\eta' \rightarrow \gamma\rho$ .

## VII. RESULTS

Table I shows the branching fractions of the two channels into their different decay modes; the first error is statistical and the second is systematic. The results for the different decay modes in the same channel are consistent within errors and are combined after taking out the common systematic errors (8.37 % for the  $\eta$  mode and 10.8% for the  $\eta'$  mode):

$$\begin{aligned} Br(J/\psi \rightarrow p\bar{p}\eta) &= (1.91 \pm 0.17) \times 10^{-3}, \\ Br(J/\psi \rightarrow p\bar{p}\eta') &= (2.00 \pm 0.36) \times 10^{-4}. \end{aligned}$$

In comparison with previous measurements of  $J/\psi \rightarrow p\bar{p}\eta$  and  $J/\psi \rightarrow p\bar{p}\eta'$ , the present results are of higher precision.

Using the result of  $J/\psi \rightarrow p\bar{p}\eta$  from this analysis and that of  $J/\psi \rightarrow p\bar{p}$  in Ref. [16], we determine:

$$\frac{\Gamma(J/\psi \rightarrow p\bar{p}\eta)}{\Gamma(J/\psi \rightarrow p\bar{p})} = 0.85 \pm 0.08.$$

TABLE II: Summary of systematic errors; “-” means no contribution.

Sources	Relative error (%)			
	$\eta \rightarrow 2\gamma$	$\eta \rightarrow \pi^+\pi^-\pi^0$	$\eta' \rightarrow \pi^+\pi^-\eta$	$\eta' \rightarrow \gamma\rho^0$
MDC tracking	4	8	8	8
Photon detection efficiency	4	4	4	2
Particle ID	$\sim 1$	4.1	4.6	3.6
Photon ID	2.0	1.6	1.6	1.6
Kinematic fit	4.0	4.0	5.0	4.0
Background uncertainty	$\sim 1$	3.1	7.3	5.8
Hadronic Interaction Model	$\sim 0$	1.4	1.4	5.2
Intermediate decay Br. Fr.	$\sim 1$	1.2	3.1	3.1
$\pi^0$ selection	-	$\sim 1$	-	
$\rho$ selection	-	-	-	5.9
Intermediate resonances	3.0	4.0	2.0	7.1
Number of $J/\psi$ events	4.7	4.7	4.7	4.7
Total systematic error	9.3	12.9	14.8	16.6

This is consistent with the calculation based on the soft-pion theorem, and indicates that the contribution of  $N^*$ - pole diagram is dominant for the  $J/\psi \rightarrow p\bar{p}\eta$  mode.

### VIII. ACKNOWLEDGMENTS

The BES collaboration thanks the staff of BEPC and computing center for their hard efforts. This work is supported in part by the National Natural Science Foundation of China under contracts Nos. 10491300, 10225524, 10225525, 10425523, 10625524, 10521003, 10821063, 10825524, the Chinese Academy of Sciences under contract No. KJ 95T-03, the 100 Talents Program of CAS under Contract Nos. U-11, U-24, U-25, and the Knowledge Innovation Project of CAS under Contract Nos. U-602, U-34 (IHEP), the National Natural Science Foundation of China under Contract No. 10225522 (Tsinghua

University), and the Department of Energy under Contract No. DE-FG02-04ER41291 (U. Hawaii).

---

- [1] P. Wang, C. Z. Yuan, X. H. Mo, *Phys. Rev. D* **70** (2004) 114014.
- [2] Rahul Sinha and Susumu Okubo, *Phys. Rev. D* **30** (1984) 2333.
- [3] L. Köpke and N. Wermes, *J/ψ Decays*, CERN, CH-1211 Geneva 23 Switzerland.
- [4] L. Adler and R. F. Dashen, *Current Algebra and Application to Particle Physics* (Benjamin, New York, 1968); B. W. Lee *Chiral Dynamics* (Gordon and Breach, New York, 1972).
- [5] J. Z. Bai *et al.*, *Nucl. Instrum. Meth. A* **458** (2001) 627.
- [6] CERN Application Software Group, GEANT Detector Description and simulation Tool, CERN Program Library Writeup W5013, Geneva (1994).
- [7] M. Ablikim *et al.*, *Nucl. Instrum. Meth. A* **552** (2005) 344.
- [8] J. C. Chen *et al.*, *Phys. Rev. D* **62** (2000) 034003.
- [9] J. Z. Bai *et al.*, *Phys. Lett. B* **510** (2001) 75.
- [10] M. Ablikim *et al.*, *Phys. Rev. D* **71** (2005) 032003.
- [11] M. Ablikim *et al.*, *Phys. Rev. D* **74** (2006) 012004.
- [12] J. Z. Bai *et al.*, *Phys. Rev. D* **70** (2004) 012005.
- [13] Particle Data Group, C. Amsler *et al.*, *Phys. Lett. B* **667** (2008) issue 1-5.
- [14] M. Ablikim *et al.*, *Phys. Rev. Lett.* **95** (2005) 262001.
- [15] S. S. Fang *et al.*, *High Energy Phys. Nucl. Phys.* **27** (2003) 277 (in Chinese).
- [16] J. Z. Bai *et al.*, *Phys. Lett. B* **591** (2004) 42.